Reaction Losses of 300 MeV Protons in a Stacked CsI(T1) Detector

AUTHOR(S):

Kakigi, Shigeru; Hayashi, Toshiharu; Okihana, Akira; Konishi, Takehiko; Fukunaga, Kiyoji; Sekioka, Tsuguhisa; Koori, Norihiko

CITATION:

Kakigi, Shigeru ...[et al]. Reaction Losses of 300 MeV Protons in a Stacked CsI(T1) Detector. Bulletin of the Institute for Chemical Research, Kyoto University 1993, 71(1): 48-56

ISSUE DATE:

1993-03-31

URL:

http://hdl.handle.net/2433/77490

Bull. Inst. Chem. Res., Kyoto Univ., Vol. 71, No. 1, 1993

Reaction Losses of 300 MeV Protons in a Stacked CsI(Tl) Detector

Shigeru KAKIGI*, Toshiharu HAYASHI*, Akira OKIHANA**, Takehiko KONISHI**, Kiyoji FUKUNAGA***, Tsuguhisa SEKIOKA† and Norihiko KOORI††

Received February 9, 1993

A stack detector consisting of six CsI(Tl) scintillators, each 3.5 cm thick, was constructed to detect protons up to 300 MeV. The detector test was performed using a 300 MeV proton beam from the ring cyclotron at the RCNP. The $\Delta E-E$ method was used to identify the events corresponding to protons undergoing nuclear reactions in the detector. For 230 MeV protons, the observed nuclear absorption rate was consistent with that calculated using the total reaction cross sections on the nuclei Cs and I, from which the efficiency was deduced to be 70%.

KEY WORDS: CsI(Tl) Sscintillator/ Stack Detector/ Efficiency

1. INTRODUCTION

In moderate resolution coincidence experiments for few-nucleon systems with beams from the ring cyclotron at the Research Center for Nuclear Physics (RCNP) of Osaka University, the large acceptance spectrograph can be used to detect charged particles of higher energies (up to 400 MeV for protons) and, on the other hand, it is necessary to prepare a full-energy detector for charged particles of lower energies (up to 300 MeV for protons). The full-energy detector for light charged particles of medium energies consists of thick materials. In this case, a considerable number of particles penetrating the detector undergoes nuclear reactions and corresponding pulse heights from the detector are anomalously small compared with those of full-energy loss.[1–5] Thus it is necessary to identify an event of a pulse height whether as due to a particle of the corresponding energy ("good" event) or as due to a higher energy particle undergoing a nuclear reaction ("bad" event). For the event identification, the detector is divided into a number of laminae (stack detector) and the $\Delta E-E$ technique is used with pulse heights from each of the detectors.[6–8]

2. DETECTOR DESIGN

Fig. 1 shows a schematic diagram of the detector. It consists of a stack of six CsI(Tl)

* 柿木 茂, 林 俊治 : Institute for Chemical Research, Kyoto University, Uji Kyoto 611.
** 沖花 彰, 小西毅彦 : Kyoto University of Education, Kyoto 612.
*** 福永清二 : Yamagata University, Yamagata 990.
† 関岡嗣久 : Himeji Institute of Technology, Himeji 671-22.
†† 桑折範彦 : Tokushima University, Tokushima 770.

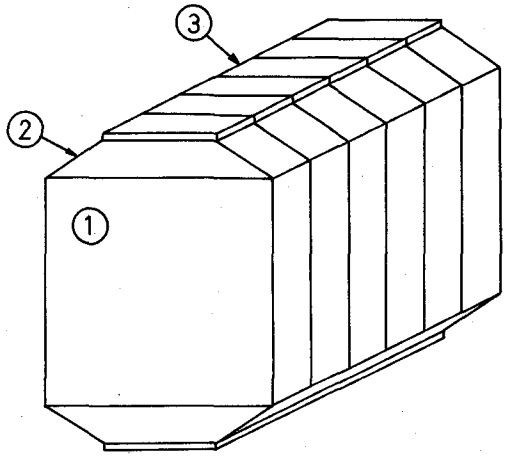

Fig. 1. Schematic diagram of the stack detector showing (1) CsI(Tl) scintillators, (2) light guides and (3) photodiodes.

scintillators ($\rho=4.51$ g/cm^3), each having a cross section of 6×6 cm^2 and a thickness of 3.5 cm. The overall thickness of 21 cm is enough to stop 300 MeV protons in the stack detector. For each scintillator, two 2.8×2.8 cm^2 photodiodes (Hamamatsu S3584-03, 300 μm wafer thichness type) are attached to the opposite faces (top and bottom) respectively through plastic light guides. Each of the light guides has a thickness of 1.5 cm with an entrance end of 6×3.5 cm^2, attached to the scintillator and an exit one of 3.5×3.5 cm^2 to which the photodiode is coupled. The light guides were introduced on the result of the test concerning the dependence of pulse heights on the incident position.[9] All the optical contacts were done with transparent grease. Each detector is contained in a cylindrical case of aluminum having an inner diameter of 11 cm with two windows of 8 cm in diameter. Gaps between the wall of the case and the detector besides around the photodiodes are filled with teflon blocks which provide mechanical contact and light reflection. Six detectors are joined into a stack detector. Between the adjacent CsI(Tl) scintillators exists a dead layer consisting of a 15 μm Al optical isolation foil and a 4 mm air gap. The output lines of two photodiodes coupled to each of the scintillators are connected togather to an input of a preamplifier (Kokendenshi KPA121A modified) followed by a linear amplifier. Output signals from six amplifiers are fed into a data acquisition system. For convenience, six components are numbered in the order from the front to the rear.

3. EXPERIMENTAL PROCEDURE AND RESULTS

The test of the stack detector was performed using a 300 MeV proton beam from the ring cyclotron at the RCNP. The beam was led into the WN line. An 1 mm thick plastic sheet was set in a target chamber for a beam polarimeter. The stack detector was set in such a way that its axis was along the direction of 25° and its front face was at a distance of 170 cm from the target. Two plastic scintillators, each of 1 cm thick and of 4×20 cm^2 area, were placed in front of the stack detector, with the overlapped area of 1×1 cm^2 and its center position set in the direction of 25°. Their coincidence signals were used as gate signals for a data acquisition system, to which output signals from six amplifiers were fed. Thus the incident position and the area of the beam

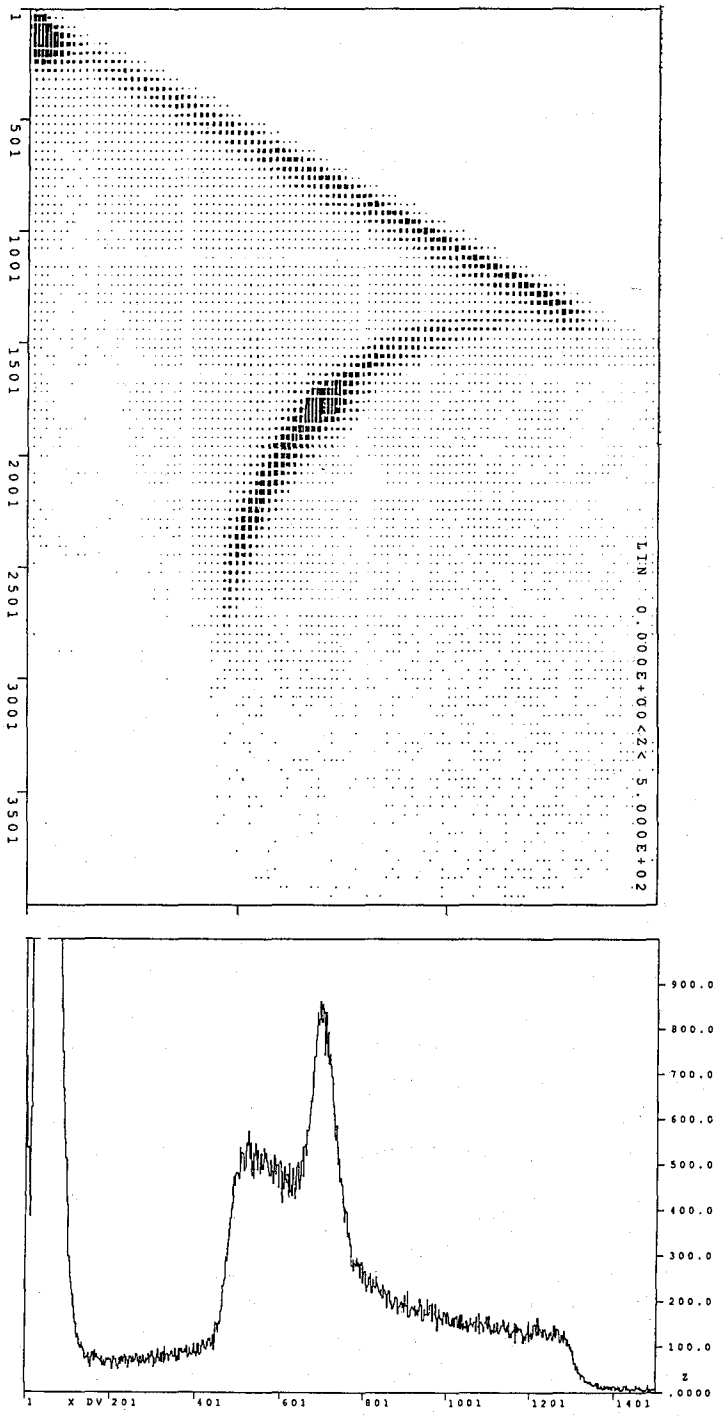

Fig. 2. $\Delta E-E$ scatter plot and projected energy spectrum. The x-axis represents the pulse height of the output signal Δ_3 from the third scintillator and the y-axis of the upper part the sum $\Delta_3+\Delta_4+\Delta_5+\Delta_6$.

spot on the detector were defined for the aquired data. The shaping time of each amplifier was set at 3 μs.

Protons scattered from the target passed through a thin Mylar window of the target chamber, then made a flight of 150 cm in air and finally passed through two plastic counters before entering the stack detector. Fig. 2 shows an energy spectrum obtained for the third CsI(Tl) scintillator, as an example. The upper part of the figure represents a $\Delta E-E$ scatter plot. The x-axis, common to two parts of the figure, represents Δ_3 and the y-axis for the upper part the sum $\Delta_3+\Delta_4+\Delta_5+\Delta_6$, where Δ_i is the pulse height of the output signal from the i-th CsI(Tl) scintillator. The spectrum shown in the lower part were obtained by projecting the yields in the $\Delta E-E$ plot onto the x-axis. An edge observed at 1340 channels corresponds to the maximum energy deposited in a single CsI(Tl) scintillator by protons, that is about 106 MeV. Each amplifier gain was adjusted in such a way that the edge appeared at about the same channel numbers. Fine adjustments were made in off-line analyses. A peak at 690 channels corresponds to protons scattered from ^{1}H target at 25°, of which energy was 240 MeV. These protons had an energy of 231 MeV after passing through two plastic counters and deposited an energy of 57 MeV in the third CsI(Tl) scintillator and stopped in the fourth one with full energy loss. An edge at 510 channels corresponds to proton groups scattered from ^{12}C, with the deposited energy of about 41 MeV. A rapid rising up of countings at very low energies may be due to background γ-rays.

Fig. 3 shows the spectra of protons penetrating the first scintillator. The upper part of the figure shows the $\Delta E-E$ scatter plot. The x-axis represents the sum of six pulse heights, approximately equal to the incident energy for the stack detector and the y-axis the pulse height Δ_1. The lower part shows the spectrum projected onto the x-axis. The events were selected on the condition that the signals from the first and the second scintillators existed. A sharp peak at 2800 channels is due to protons elastically scattered from the ^{1}H target and associated events observed in the upper part at lower energies with almost constant Δ_1 correspond to protons undergoing nuclear reactions in the following scintillators. An edge observed at 1450 channels corresponds to the minimum energy of which protons can penetrate the first scintillator, that is 106 MeV. A part of the "bad" events appears lower than the edge in the figure. Then the penetration condition was changed in order and five spectra were obtained. They are shown in Fig. 4. The spectrum labeled 1 was obtained without event selection. The labeled 2 is the same as the spectrum in Fig. 3. The labeled 3 was obtained on the penetration condition that the signals from the first, the second and the third scintillators existed and so forth.

4. DISCUSSION

An event can be identified as "good" or "bad" with the $\Delta E-E$ method[7,8] using the empirical formula for the range-energy relation,

$$R(E)=aE^b,$$

where the parameter a depends on the particle type and b is almost constant taking the value of 1.73. Then the following relation is obtained.

$$R(E)=nw+R(E-\Delta E),$$

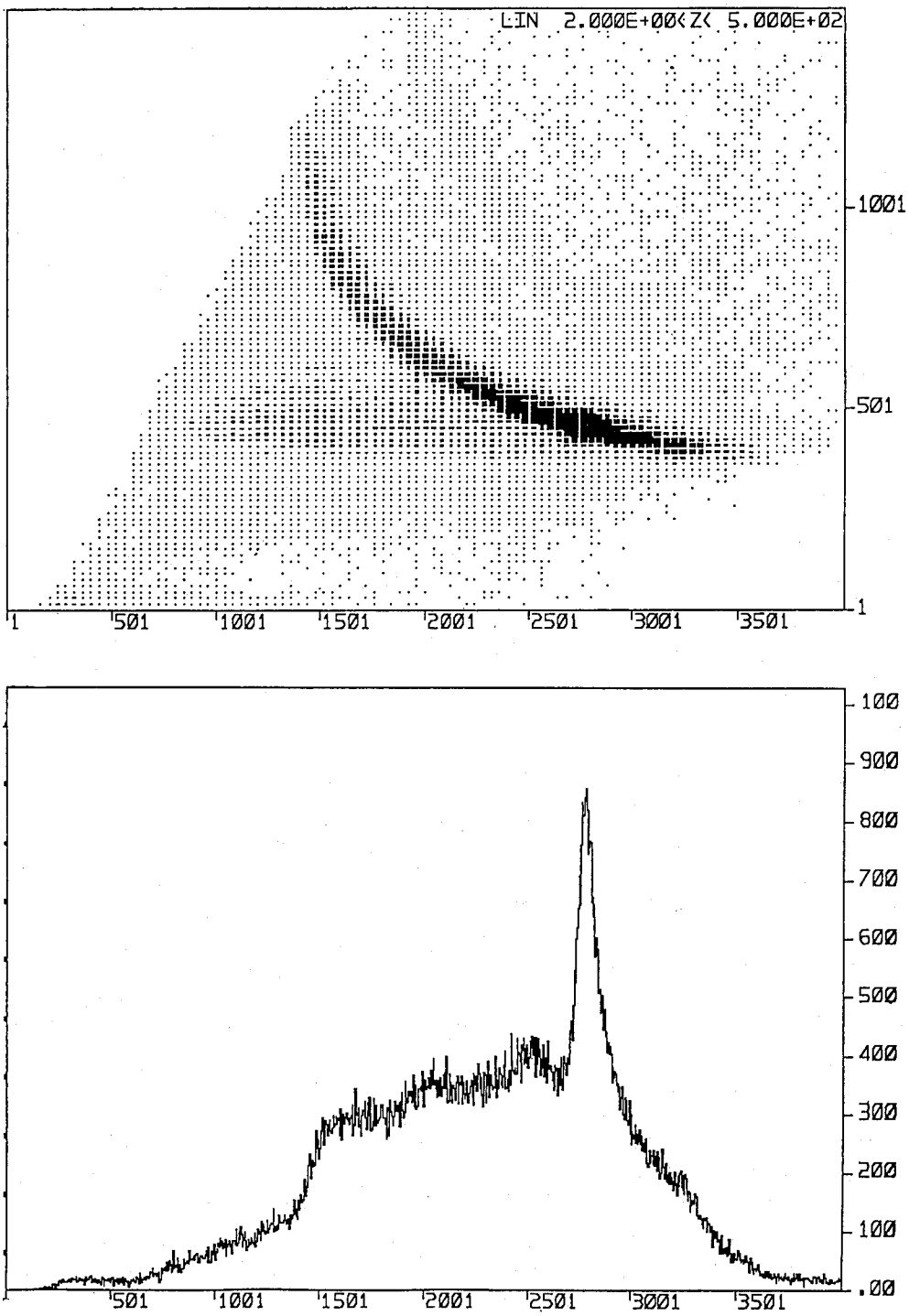

Fig. 3. $\Delta E-E$ scatter plot and projected energy spectrum. The x-axis represents the sum $\Delta_1+ \ldots +\Delta_6$ and the y-axis of the upper part Δ_1. For the event selection see the text.

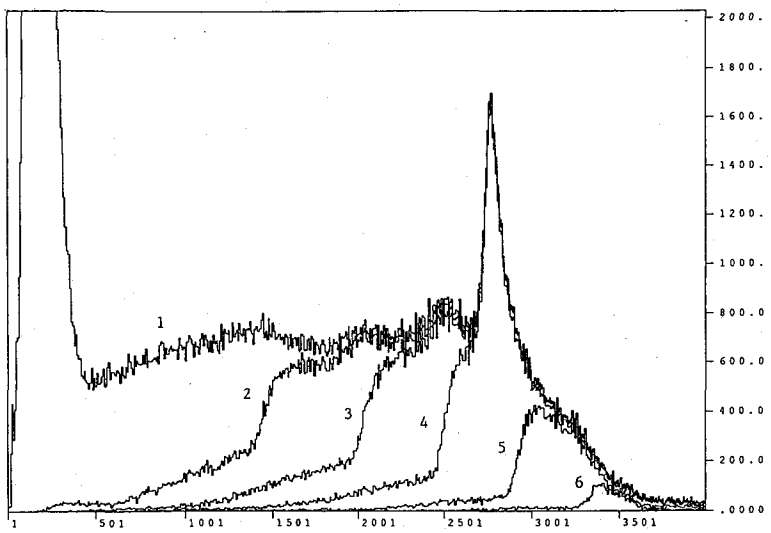

Fig. 4. Energy spectra obtained on the different penetration conditions.

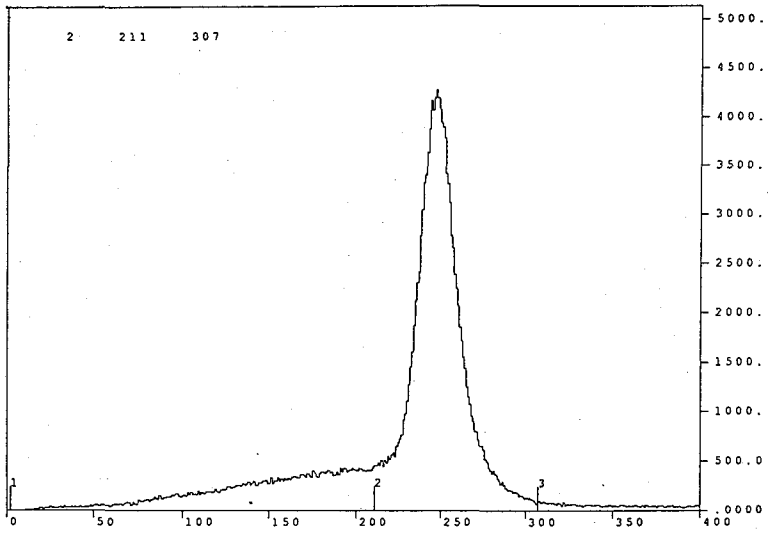

Fig. 5. Particle spectrum. The peak corresponds to protons of full-energy loss and the tail to those undergoing nuclear reactions in the detector.

where E is the incident energy and ΔE the ionization energy loss in the first n scintillators of the total thickness nw. The particle parameter P defined by $P=w/a$ is equal to

$$P=[E^b-(E-\Delta E)^b]/n.$$

Fig. 5 shows a particle (P) spectrum obtained for $\Delta E=\Delta_1$. The peak corresponds to protons of full-energy loss ("good" events) and the tail to those undergoing nuclear reactions ("bad" events). The division point between peak and tail regions was set at 210 channels.

To select events corresponding to protons elastically scattered from ^{1}H, a window was set for the $\Delta E-E$ scatter plot. For example, the Δ_1 window width was from 390 to 490 channels for

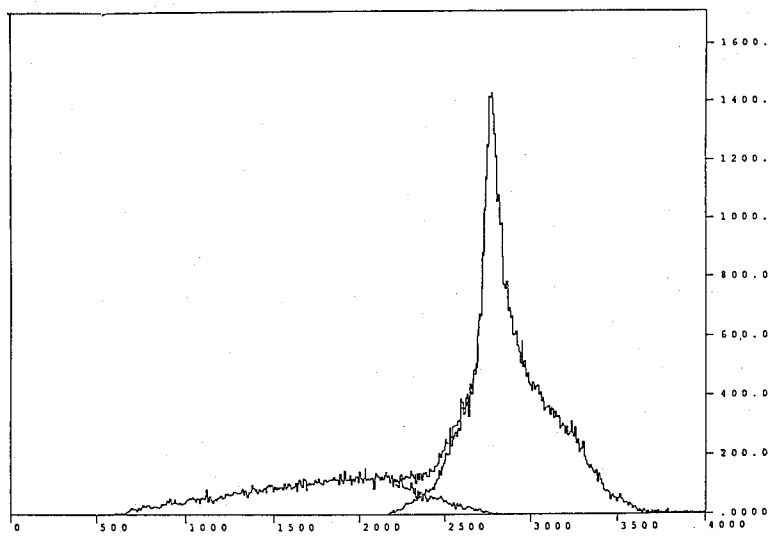

Fig. 6. Energy spectra obtained by setting the Δ_1 and P windows.

the plot in Fig. 3. The obtained spectrum is shown in Fig. 6 together with two spectra (of "peak" and "tail" regions) obtained by setting the additional window for the P spectrum. A bump at the higher energy side of the peak was due to protons scattered from ^{12}C which were confused owing to large width of the Δ_1 window. The same procedure was done for the spectra labeled 3

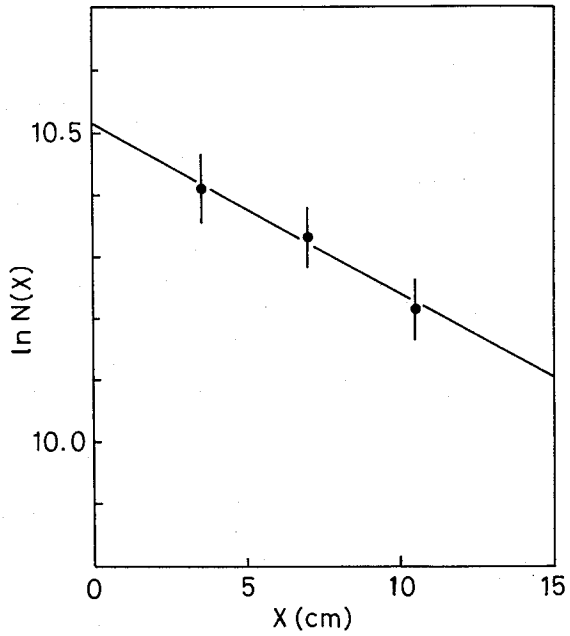

Fig. 7. Number of protons as a function of the penetration thickness x. The line corresponds to the absorption coefficient of 0.027 cm^{-1} calculated from the total reaction cross sections on the nuclei Cs and I.

and 4 shown in Fig. 4. The numbers of counts $N_G(x)$ for the "good" events and $N_B(x)$ of the "bad" events were obtained for protons penetrating the first ($x=3.5$), the second ($x=7.0$) and the third ($x=10.5$) CsI(Tl) scintillators, respectively, where the values of x (in cm) are the distance of the scintillator boundary from the front surface of the stack detector. The number of counts $N_G(x)$ should be independent of x because the corresponding protons penetrate the first three scintillators and stop in the fourth one with full-energy loss. The observed numbers of counts $N_G(x)$ were different owing to the different widths of the windows used for three cases and the first two counts were normalized to the third one. The observed numbers of counts $N_B(x)$ were multiplied by the same factors as for $N_G(x)$. The number of protons $N(x)=N_G(x)+N_B(x)$ was obtained from these data as a function of x and is shown in Fig. 7. The number of protons after penetrating a thickness x is given by

$$N(x)=N_0 \exp(-\mu x),$$

where μ is the absorption coefficient, assumed to be constant. The coefficient μ is given by

$$\mu=[\sigma(\mathrm{Cs})+\sigma(\mathrm{I})]\ \rho N/A,$$

where σ is the total reaction cross section for protons on the nucleus Cs or I, ρ is the density of CsI (4.51 g/cm^3), A is the molecular weight of CsI (260)[4] and N is the Avogadro's number (6.023×10^{23} atoms/mol). An assumption that $\sigma(\mathrm{Cs})=\sigma(\mathrm{I})$ was taken because the values of (Z, A) for Cs and I are nearly equal. In addition, was assumed that σ is almost constant for proton energies higher than about 100 MeV. Finally $\mu=0.027$ cm^{-1} was obtained using σ of about 1.3 b [5] and the corresponding line is shown in Fig. 7. The experimental result is well reproduced. The value $N_0=3.3\times10^4$ was obtained from the fit to the data. The range $R=13.3$ cm is obtained from the data[10] by interpolation for the protons elastically scattered from ^{1}H target which have the energy of 231 MeV at the entrance of the stack detector. Using this value the efficiency is calculated to be $\exp(-0.027\times13.3)=0.70$.

To use the stack detector in nuclear reaction experiments, several problems should be noticed. One of them is concerning γ-ray backgrounds. When they are more intense, it is more probable that γ-ray signals are accidentally accepted in the data acquisition system instead of particle ones. These events are treated as "bad" ones and the efficiency of the detector decreases. Thus the detector should be sufficiently shielded from γ-rays. Next, if "bad" events are rejected from the data, the correction of countings is necessary as a function of the particle energy to obtain absolute values of cross sections. However, it is troublesome, in particular, in coincidence experiments. To revive "bad" events, the particle full energy can be reconstructed from the energies deposited in the detectors preceding the one in which nuclear reaction occurs, although the energy resolution decreases.

This experiment was performed at the RCNP under Program Numbers 32A102 and 33A110.

REFERENCES

(1) J.M. Cameron, P. Kitching, R.H. McCamis, C.A. Miller, G.A. Moss, J.G. Rogers, G. Roy, A.W. Stetz, C.A. Goulding and W.T.H. van Oers, *Nucl. Instr. and Meth.*, **143**, 399 (1977).

(2) A. Bracco, H.P. Gubler, D.K. Hasell, W.T.H.van Oers, R. Abegg, C.A. Miller, M.B. Epstein, D.A. Krause, D.J. Margaziotis and A.W. Stetz, *Nucl. Instr. and Meth.*, **219**, 329 (1984).

(3) A.M. Sourkes, M.S. de Jong, C.A. Goulding, W.T.H. van Oers, E.A. Ginkel, R.F. Carlson, A.J. Cox and D.J. Margaziotis, *Nucl. Instr. and Meth.*, **143**, 589 (1977).
(4) D.F. Measday and C. Richard-Serre, *Nucl. Instr. and Meth.*, **76**, 45 (1969).
(5) C.A. Goulding and J.G. Rogers, *Nucl. Instr. and Meth.*, **153**, 511 (1978).
(6) M. Makino, R. Eisberg, K. Richie, R. Carlson and C. Waddell, *Nucl. Instr. and Meth.*, **80**, 299 (1970).
(7) M. Makino, R. Eisberg, D. Ingham and C. Waddell, *Nucl. Instr. and Meth.*, **81**, 125 (1970).
(8) R. Eisberg, M. Makino, R. Cole, C.N. Waddell, M. Baker, J.J. Jarmer, D.M. Lee and P. Thompson, *Nucl. Instr. and Meth.*, **146**, 487 (1977).
(9) S. Kakigi, K. Fukunaga, T. Hayashi, A. Okihana, T. Konishi and T. Sekioka, *Bull. Inst. Chem. Res., Kyoto Univ.*, **70**, 10 (1992).
(10) J.M. Paul, *Nucl. Instr. and Meth.*, **96**, 539 (1971).